JOURNAL OF SPACECRAFT AND ROCKETS
Vol. 41, No. 4, July–August 2004

Shape Achievement of Optical Membrane Mirrors Using Coating/Substrate Intrinsic Stresses

J. T. Ash* and C. H. Jenkins†
South Dakota School of Mines and Technology, Rapid City, South Dakota 57701
and
D. K. Marker‡ and J. M. Wilkes‡
U.S. Air Force Research Laboratory, Kirtland Air Force Base, New Mexico 87117-5776

The U.S. Air Force, as well as many other organizations, has evinced considerable interest in developing large gossamer membrane radio antennas and optical quality telescopes. A concept is discussed of global shape maintenance of a reflective polymer membrane element after curing, coating, and release from a precision casting mold of the desired parabolic shape. The idea involves manipulation of intrinsic stresses in the coating and its membrane substrate. Results from an axisymmetric, geometrically linear, shallow-shell theory are presented as closed-form solutions for the displacement fields. A unique condition emerges from these solutions, suggesting that zero deformations can occur in a 0-*g* environment. Results of a finite element analysis are presented, showing that if a coated membrane satisfying this condition is subjected to a 1-*g* loading, rms errors of 9.3 μm and 2.8 mm can be expected for 1- and 20-m-diam mirrors, respectively. However, in the case of a 1-*g* load, another condition follows from the theory, which, if met, predicts zero deformation in the 1-*g* environment. Additional results of the finite element analysis are presented that lend support to these conclusions.

Nomenclature

A	=	material parameter of coated membrane laminate, $(h_c Q_c + h_s Q_s)$, N/m
A_ν	=	material parameter of coated membrane laminate, $(h_c Q_c \nu_c + h_s Q_s \nu_s)$, N/m
a	=	radius of circular aperture, m
B	=	material parameter of coated membrane laminate, $[\frac{1}{2} h_c h_s (Q_c - Q_s)]$, N
B_ν	=	material parameter of coated membrane laminate, $[\frac{1}{2} h_c h_s (Q_c \nu_c - Q_s \nu_s)]$, N
C_1, C_2, C_3	=	integration constants in displacement component solutions, m
D	=	material parameter of coated membrane laminate, $\{\frac{1}{12}[(h_c^3 + 3h_c h_s^2) Q_c + (h_s^3 + 3h_s h_c^2) Q_s]\}$, N · m
E_c	=	elastic modulus of coating, N/m^2
E_s	=	elastic modulus of membrane, N/m^2
$F^\#$	=	f number of initial paraboloidal shape, $f/(2a)$
f	=	focal length of initial paraboloidal shape, m
g	=	gravitational acceleration at Earth's surface, 9.81 m/s^2
h_c	=	coating thickness, m
h_s	=	membrane thickness, m
k_2	=	parameter in argument of Kelvin functions, 1/m, $\left(\left\{\left(\frac{1}{4f^2}\right)\left[\frac{(A + A_\nu)(A - A_\nu)}{AD - B^2}\right]\right\}^{\frac{1}{4}}\right)$
N_0	=	stress resultant load factor, N/m
p_{11}, p_{12}	=	dimensionless boundary condition coefficients
Q_c	=	material parameter $E_c/(1 - \nu_c^2)$ of coating, N/m^2
Q_s	=	material parameter $E_s/(1 - \nu_s^2)$ of membrane, N/m^2
R	=	radial coordinate, $0 \le R \le a$, m
r^2	=	statistical coefficient of determination
S_c	=	coating intrinsic stress, N/m^2
S_s	=	membrane intrinsic stress, N/m^2
$u(a)$	=	radial displacement component at edge, m
$u(R)$	=	radial displacement component, m
$u(0)$	=	radial displacement component at center, m
u_1	=	constant in radial displacement solution, m^4
u_2	=	constant in radial displacement solution, m
$w(a)$	=	axial displacement component at edge, m
$w(R)$	=	axial displacement component, m
$w(0)$	=	axial displacement component at center, that is, apex displacement, m
α_c	=	coating coefficient of thermal expansion (CTE), m/m · K
α_s	=	membrane CTE, m/m · K
$\Gamma(R)$	=	function defining initial paraboloidal shape of coated membrane, m
ΔT	=	temperature difference, K
ε_c	=	coating thermal strain, $\alpha_c \Delta T$, m/m
ε_s	=	membrane thermal strain, $\alpha_s \Delta T$, m/m
ν_c	=	coating Poisson's ratio
ν_s	=	membrane Poisson's ratio
ρ_c	=	coating mass density, kg/m^3
ρ_s	=	membrane mass density, kg/m^3

Subscripts

c	=	coating
s	=	membrane substrate

Introduction

IN the context of spacecraft, gossamer signifies ultralightweight systems with high packaging efficiency. Given the fixed launch allowables for mass and volume, large apertures (perhaps larger than 8–10 m) will have to be gossamer. The development of space-based gossamer membrane reflectors with diameters in excess of 8 m has been pursued since the deployment of the Echo series of balloons in the early 1960s. Echo I consisted of a number of 12.7-μm-thick

Received 31 July 2002; revision received 15 July 2003; accepted for publication 15 July 2003.

*Ph.D. Student, Compliant Structures Laboratory, Mechanical Engineering Department. Member AIAA.
†Professor and Head, Compliant Structures Laboratory, Mechanical Engineering Department. Member AIAA.
‡Senior Technical Advisor, Directed Energy Directorate/Surveillance Technologies Branch, 3550 Aberdeen Avenue Southeast.

aluminized Mylar® gores bonded together to form a 30.5-m-diam balloon.[1] Echo was successfully used for a number of months as a passive radio reflector to transmit audio and television signals, as well as to broadcast a message from President Eisenhower across the nation.

Like the Echo series and its many successors, the design of gossamer membrane reflectors has emphasized the inflatable lenticular concept. The inflatable lenticular consists of a highly reflective coated polymer substrate and a transparent canopy joined at the outer edge by an inflatable torus. When inflated, the reflective membrane surface serves as the primary reflecting element, as the wavefront makes a double pass through the transparent canopy to the collecting element. The inflatable torus serves as the support structure for the reflector and is tied to the space satellite by means of inflatable struts. This paper focuses on the development of membrane reflectors by methods different from the inflatable paradigm and investigates a novel idea of using intrinsic stresses in the coating and substrate as a means of maintaining a near net-shape mirror without the requirement for a transparent canopy.

Researchers at the U.S. Air Force Research Laboratory (AFRL), Directed Energy Directorate, have undertaken the task of developing an optical quality gossamer membrane mirror for space-based applications. A summary of their research toward this end, current to approximately midyear 2000, can be found in Ref. 2. Interest in such technology is driven by the requirement for an overwhelming improvement in resolving power of the primary optical element, that is, in reducing the minimum transverse distance between two object points that can just be resolved. Traditional rigid optics are essentially eliminated from this gossamer class of mirrors by both their overall mass and their size. Although membrane materials will satisfy the mass and size constraints when packaged, launched, and then deployed, the manufacture of an optical quality membrane telescope is a challenging task. First, the surface precision of the reflecting element has to be on the order of 1/20th the wavelength of interest, which when considering the visible light spectrum between 400 and 760 nm places a constraint of 20 nm on the surface precision. When conventional adaptive optics techniques are used, this constraint can be relaxed to several micrometers; for example, see Ref. 2, pp. 158–160. Diffractive wavefront control based on real-time holographic phase subtraction will further relax the surface precision requirement to approximately 100 μm (Refs. 3–5). At present, neither technique will correct for either high spatial frequency aberrations, or for scattering of light due to surface roughness at the microscale. Consequently, optical quality membranes must be manufactured with an extremely high degree of surface smoothness. Finally, when considering such factors as packaging, deployment, thermal deformation, and surface degradation due to the extreme environment of space, it is unlikely that any passive method will be successful in maintaining the desired shape over the mission life. Therefore, some active control scheme is required to fine-tune the shape of the mirror.

Research has verified that thickness variations in the transparent canopy of an inflatable lenticular would likely be significant enough to perturb the flow of optical information beyond the means of adaptive optics corrective techniques.[6] Although the lenticular concept has by no means been abandoned, investigations were begun of alternative near net-shape membrane technologies that do not require the use of a transparent canopy. One possibility is the use of shape memory alloys to force the membrane into the desired shape. Other possibilities include placing electrostatic, electrostrictive or bimorphic elements on the membrane such that, when an electric field, electron beam, or light beam is utilized, the materials are activated and assume the predetermined shape.

In addition to these methods, it was observed that some substrate films were deformed from their original planar configuration after the deposition of a coating. Initially, it was assumed that thermal effects caused the deformation, but coating experts later identified the cause as an intrinsic stress state in the coating induced during the deposition process. This observation led to the present consideration of using these coating stresses as a means of either obtaining the parabolic shape or maintaining the shape of an already parabolic membrane substrate after removal from the parabolic mold on which it was cast.

Thin-film coatings have long been known to produce an initial stress state when deposited using the sputtering, evaporation, or electroplating processes. When deposited upon thicker substrates, only slight induced curvature results from the intrinsic stress. Stoney[7] observed this in 1909 when he was attempting to protect silver films deposited on glass searchlight reflectors. Electroplating the silver film with a layer of copper, he found that if the thickness of the copper exceeded 10 μm, both the copper coating and silver film were liable to peel off together. This observation led to the derivation of Stoney's equation, which provided a simple expression for the intrinsic stress in terms of the curvature imparted to the thin-steel beam. Brenner and Senderoff[8] later derived three separate equations resulting from different boundary conditions during the deposition process and relaxed some of the assumptions used in Stoney's derivation. Harper and Wu[9] used classical laminate theory to solve the geometrically linear problem for a rectangular plate free of external constraints and, following the seminal work of Hyer,[10] obtained geometrically nonlinear approximate solutions. Their work[9] uses the Kirchhoff–Love assumptions from classical plate theory, postulates simple parametric forms for the displacement components, and then minimizes the strain energy to determine optimal values for the parameters. Masters and Salamon[11] extended the geometrically nonlinear approximate solutions by sequentially eliminating some of the restrictions in the strain fields, resulting in a lower energy solution.

The majority of the work conducted on the derivation of coating stress as a function of induced curvature relates to initially planar configurations. Where this is not the case, superposition is often used by subtracting out the initial curvature from the final curvature.[12] Fahnline[13] presented two equations derived by the energy minimization method, but more appropriately accounted for an initial substrate curvature by including an additional stress field in the total strain energy to be minimized.

Another important factor to consider is that polymer membranes have been observed to exhibit a curing strain as a result of polymer linking, solvent evaporation, and thermal mismatch during the curing process.[14–16] If the polymer adheres to the surface of a mold during the curing process, this curing strain typically results in an intrinsic tensile stress in the membrane. Such stresses would cause the membrane to shrink into a stress-free state if removed before coating. However, if a coating is deposited before removing the membrane from the mold, the membrane substrate intrinsic stresses must be taken into account in addition to the coating intrinsic stresses (which may be either compressive or tensile, depending on the coating process conditions).

The goal of this work was to determine whether the shape of an initially parabolic membrane substrate could be preserved, after manufacture, coating, and removal from the casting mold, with the use of coating stresses. We do not address here the control problems associated with shape maintenance of the coated membrane after packaging, launch, and deployment. An examination of geometrically linear shallow-shell theory has been conducted for an initially curved laminate possessing intrinsic stresses in both the coating and membrane substrate. The resulting displacement field solutions are presented for the fixed-edge boundary value problem, with supporting results from a finite element analysis. It is shown in this work that a coating prescription can be given that counteracts membrane shrinkage stresses and that theoretically maintains a near net-shape gossamer membrane mirror in a 0-g environment. An alternative coating prescription can be given to maintain a parabolic mirror in a 1-g environment. Finite element results are also presented that address such factors as stress stiffening and size effects occurring as the mirror diameter is increased.

Theoretical Results

Starting from the general three-dimensional theory of elasticity, the method of asymptotic expansions was used to obtain both geometrically linear and geometrically nonlinear theories of thin laminate shells consisting of a membrane and its high-reflectance coating. A detailed account of this work has been presented elsewhere.[17]

It suffices to say here that, when specialized to axisymmetric problems, the resulting geometrically nonlinear theory is essentially that used long ago by Wittrick[18] in his classic study of the stability of a bimetallic disk thermostat. To our knowledge, no general solutions of this nonlinear theory are known.

However, for the axisymmetric, geometrically linear theory, general solutions for the displacement components have been obtained. In particular, assuming the initial configuration of the coated membrane to be a paraboloid of focal length f and aperture radius a, defined by the equation

$$\Gamma(R) = (1/4f)(a^2 - R^2) \tag{1}$$

we find[19] for the axial displacement $w(R)$ (from the initially parabolic membrane to its deformed shape), as a function of the radial coordinate R, the following linear combination of Kelvin functions:

$$w(R) = C_1\mathrm{ber}(k_2R) + C_2\mathrm{bei}(k_2R) + C_3 \tag{2}$$

where C_1, C_2, and C_3 are arbitrary integration constants. The general solution for the radial displacement $u(R)$ is complicated, involving $w(R)$ and its derivatives, but can be brought to the form

$$u(R) = u_1k_2^3[-C_1\mathrm{bei}'(k_2R) + C_2\mathrm{ber}'(k_2R)] + u_2k_2[C_1\mathrm{ber}'(k_2R) + C_2\mathrm{bei}'(k_2R)] + (1/2f)R[C_1\mathrm{ber}(k_2R) + C_2\mathrm{bei}(k_2R)] - [N_0/(A + A_\nu)]R \tag{3}$$

where for convenience we have introduced two new constants u_1 and u_2 defined by

$$u_1 = -2f\frac{(AD - B^2)}{A(A_\nu - A)}, \qquad u_2 = \frac{(AB - 2AB_\nu + A_\nu B)}{A(A_\nu - A)} \tag{4}$$

and the prime on a Kelvin function denotes a derivative with respect to the argument k_2R. The stress resultant load factor N_0 appearing in Eq. (3) will be defined shortly. Restricting attention to the boundary value problem corresponding to a rigidly clamped edge, the boundary condition $w(a) = 0$ determines $C_3 = -C_1\mathrm{ber}(k_2a) - C_2\mathrm{bei}(k_2a)$, whereas the coefficients C_1 and C_2 must be solutions of the boundary conditions $u(a) = 0$ and $w'(a) = 0$. These two conditions can be written as

$$u(a) = p_{11}C_1 + p_{12}C_2 - [aN_0/(A + A_\nu)] = 0 \tag{5}$$

$$w'(a) = k_2[C_1\mathrm{ber}'(k_2a) + C_2\mathrm{bei}'(k_2a)] = 0 \tag{6}$$

where p_{11} and p_{12} are given by

$$p_{11} = (a/2f)\mathrm{ber}(k_2a) - k_2^3u_1\mathrm{bei}'(k_2a) + k_2u_2\mathrm{ber}'(k_2a) \tag{7}$$

$$p_{12} = (a/2f)\mathrm{bei}(k_2a) + k_2^3u_1\mathrm{ber}'(k_2a) + k_2u_2\mathrm{bei}'(k_2a) \tag{8}$$

Equations (5) and (6) are easily solved, yielding

$$C_1 = \frac{aN_0}{A + A_\nu}\left[\frac{\mathrm{bei}'(k_2a)}{p_{11}\mathrm{bei}'(k_2a) - p_{12}\mathrm{ber}'(k_2a)}\right] \tag{9}$$

$$C_2 = \frac{aN_0}{A + A_\nu}\left[\frac{\mathrm{ber}'(k_2a)}{p_{11}\mathrm{bei}'(k_2a) - p_{12}\mathrm{ber}'(k_2a)}\right] \tag{10}$$

For this boundary value problem, both the radial and axial displacement solutions are observed to contain (through the constants C_1 and C_2) the common factor N_0. In the absence of a gravitational body force, which we refer to as the 0-g case, this factor is given by

$$N_0 = h_cS_c + h_sS_s \tag{11}$$

When a gravitational body force in the axial direction is present, which we refer to as the 1-g case, N_0 has the form

$$N_0 = h_cS_c + h_sS_s - 2aF^{\#}(h_c\rho_c + h_s\rho_s)g \tag{12}$$

Table 1 Material and geometrical properties

Parameter	Coating	Membrane
Thickness h, μm	1	20
Young's modulus E, GPa	44	2.2
Poisson's ratio ν	0.4	0.4
Density ρ, kg/m^3	2790	1470
CTE α, m/m · K	6×10^{-4}	-6×10^{-4}
ΔT, K	Variable	Variable

Note that the gravity load acts in the upward axial direction with the mirror's coated reflecting surface facing down, in accordance with Eq. (1). (The basis of this rather counterintuitive orientation is the optical convention that the direction of propagation of light, which strikes the coating first, coincides with the positive Z direction, which is upward in our model.) Thus, by choosing the parameters in N_0 appropriately, that is, by prescribing a compressive coating stress in the 0-g case given by

$$S_c = -(h_s/h_c)S_s \tag{13}$$

or in the 1-g case by

$$S_c = -(h_s/h_c)S_s + 2aF^{\#}[(h_c\rho_c + h_s\rho_s)/h_c]\,g \tag{14}$$

it should be possible to maintain the initial parabolic shape of the coated membrane after removal from the mold. We refer to Eqs. (13) and (14) as the ondesign coating prescriptions for 0-g and 1-g loads, respectively.

Comparisons were made between the closed-form solutions given in Eqs. (2) and (3) and finite element results. In the section that follows, we discuss the finite element modeling in detail and tabulate the material and geometrical properties used (Table 1). Here, we simply state the important results of our comparisons with the theory.

First, a 5-m radius, $f/2$ ($F^{\#} = 2$), coated membrane mirror with a 0-g ondesign coating stress prescription was modeled using the nonlinear finite element program ABAQUS. These values of a and $F^{\#}$ imply a focal length of $f = 2aF^{\#} = 20$ m and an initial apex position of $\Gamma(0) = a^2/(4f) = 0.3125$ m. The initial paraboloid then curves from this point to $\Gamma(5) = 0$ as required by Eq. (1) and is modeled by 49 elements and 99 nodes of axisymmetric shell elements with a quadratic displacement field. An 11-MPa intrinsic tensile membrane stress S_s was specified, requiring a -220-MPa intrinsic coating stress S_c to satisfy Eq. (13). The finite element analysis showed zero displacements everywhere, as predicted by the theory.

Next, to verify the theoretical expressions for the displacement fields, the same model was utilized, except that offdesign coating stresses were introduced to promote deformation. The coating stress was increased in increments of 1% of the ondesign value, up to a 10% offdesign case. Finite element analysis (FEA) was conducted using both geometrically linear and nonlinear solution schemes to determine the applicability of the geometrically linear shallow-shell theory. A FORTRAN program was written to provide a quick graphical analysis of the displacement field components given in Eqs. (2) and (3), subject to clamped edge boundary conditions. In Figs. 1 and 2, we show comparisons of the theory and FEA for a case in which the membrane has 0.3% intrinsic strain, whereas the coating stress has been chosen to be 1% higher than the ondesign prescription value of Eq. (13). Figures 3 and 4 show the same comparisons, but with a coating stress that is 10% above the ondesign value of Eq. (13). An edge-effect beginning some 10–20 cm from the edge is observed in both the theoretical and FEA results. The graphs of radial displacement pass through the origin and are linear until the onset of this edge effect, whereas the axial displacement curves are quite flat until the edge effect occurs. To enhance the detail of these edge effects, we have shown in Figs. 1–4 only the final meter before reaching the edge. The agreement between theoretical and geometrically linear FEA results in Figs. 1–4 is rather remarkable.

In Fig. 2, the geometrically nonlinear axial displacement is roughly 97% of the theoretical prediction for the 1% offdesign case, whereas in Fig. 4 the nonlinear prediction is only 72% of the theoretical one. The tendency for the theoretical result to overestimate

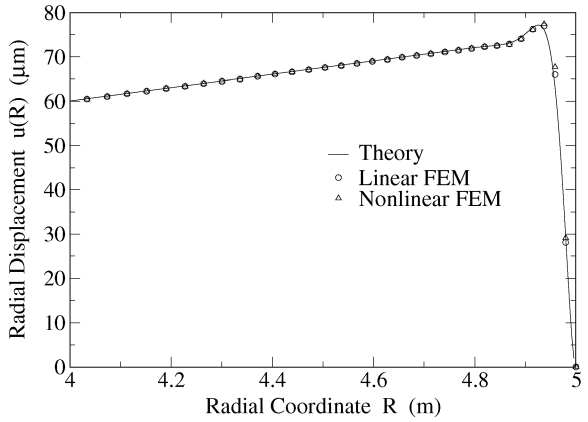

Fig. 1 Comparison of theory and finite element results for radial displacement $u(R)$ when the coating stress is 1% offdesign.

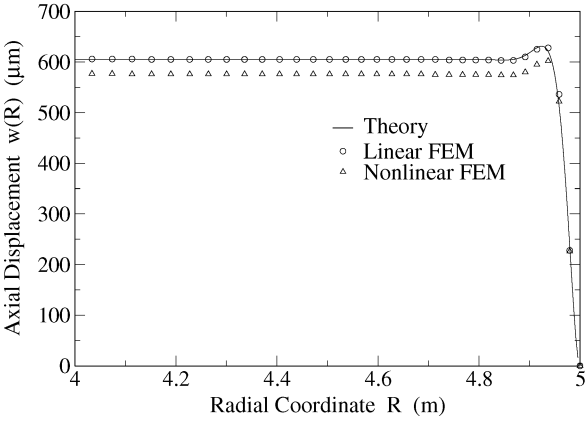

Fig. 2 Comparison of theory and finite element results for axial displacement $w(R)$ when the coating stress is 1% offdesign.

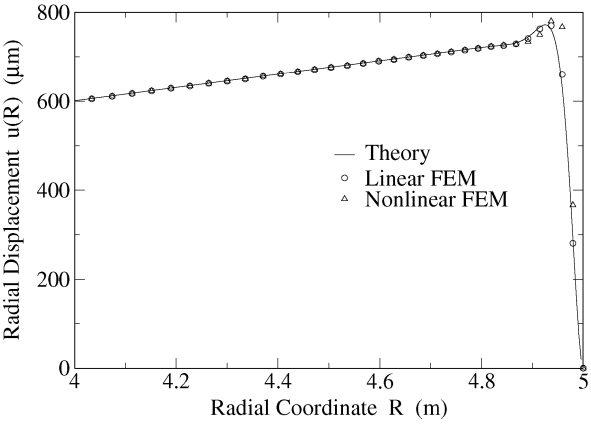

Fig. 3 Comparison of theory and finite element results for radial displacement $u(R)$ when the coating stress is 10% offdesign.

the axial displacement is evident in Fig. 5, which indicates that for this example geometrical nonlinearities become important when the coating stress is more than 2% offdesign, whereas the theory is fairly accurate when offdesign by less than 2%.

Finite Element Study

In the preceding section, ondesign coating prescriptions were proposed that would maintain the parabolic shape of a membrane mirror in either a 0-g or 1-g environment. In terms of ground testing and determining the quality of such a mirror, design for a 1-g environment would be preferred. When manufacturing a mirror for space applications, however, the membrane substrate would be coated for

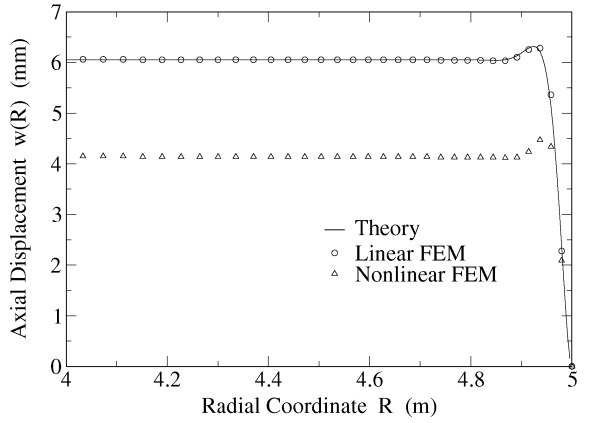

Fig. 4 Comparison of theory and finite element results for axial displacement $w(R)$ when the coating stress is 10% offdesign.

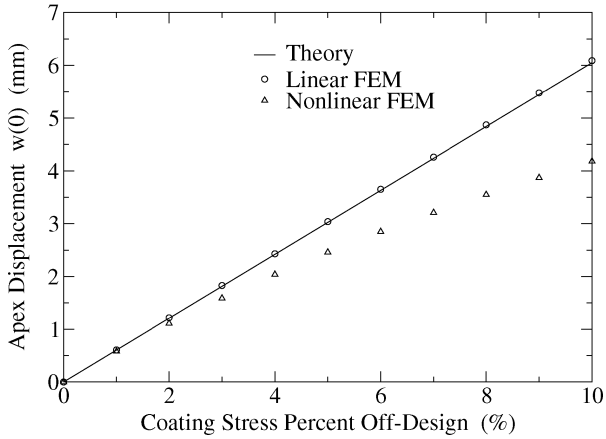

Fig. 5 Comparison of theory and finite element results for apex displacement $w(0)$ as a function of the percent that coating stress is offdesign.

use in a 0-g environment, and any ground testing before launch would have 1-g loading deformations perturbing the mirror from its ondesign 0-g configuration.

The finite element study presented here focuses on the issue of gravity sag error. The ondesign coating prescription given in Eq. (13) for a 0-g environment is enforced, and the mirror is then subjected to a 1-g body force. The manufacturer of the optical quality polymer membrane material CP1-DE (SRS Technologies, Inc., Huntsville, Alabama), used by AFRL researchers in most of their recent work, has devised processing methods that control the amount of residual stress in their membranes. In addition, researchers have demonstrated the ability to manipulate[20] the amount of intrinsic stress imparted to a coating during the coating process. The question then becomes, are there any benefits, for example, a stress-stiffening effect, of having high vs low intrinsic stress states in the coating and membrane under the conditions of an ondesign 0-g coating prescription?

To determine whether a stress-stiffening effect exists, a 20-m-diam $f/2$ mirror was modeled in ABAQUS, using axisymmetric shell elements with a quadratic displacement field and a geometrically nonlinear solution scheme. A total of 49 elements and 99 nodes were used to define the entire parabolic profile. The membrane shrinkage strain ε_s was allowed to vary from 0 to 1% in increments of 0.1%. The coating stress S_c was adjusted to satisfy Eq. (13). To determine sufficient convergence of the model, results were compared with a 197 node model, which indicated only an additional 0.2% displacement at the apex.

The boundary condition for the model is a clamped outer boundary as is required by the ondesign coating prescription. In our axisymmetric model, the apex node was allowed to translate along the axial direction and constrained from rotating, to preserve axial

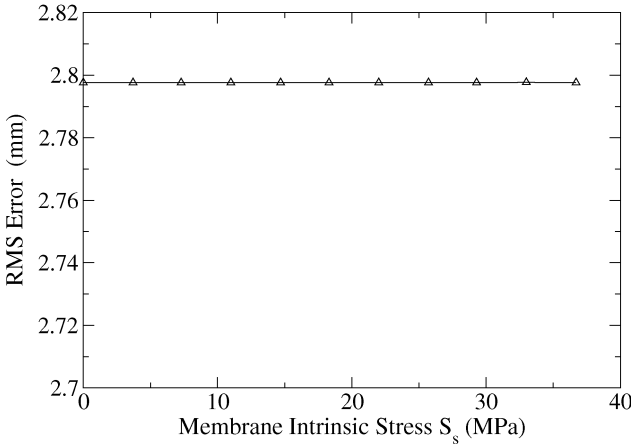

Fig. 6 RMS error of 20-m-diam, *f*/2 mirror, 0-*g* ondesign case subjected to 1-*g* gravity load (corresponding to a 7.86-mm apex deflection).

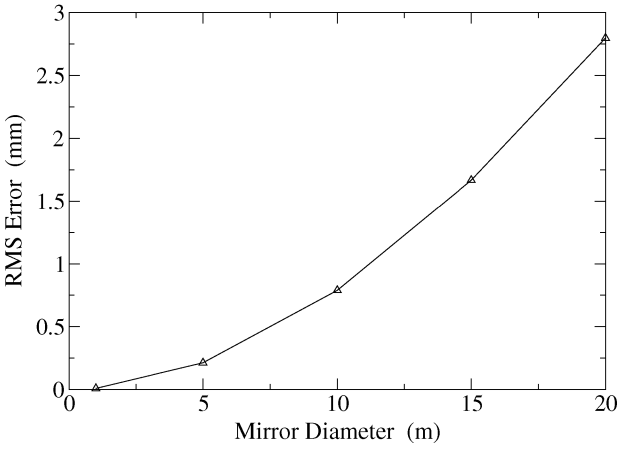

Fig. 7 Size effect for 0-*g* ondesign mirrors subjected to 1-*g* gravity load.

symmetry. The intrinsic stresses are simulated in the model by thermal stresses, that is,

$$S_c = -[E_c/(1-\nu_c)]\varepsilon_c, \qquad S_s = -[E_s/(1-\nu_s)]\varepsilon_s \quad (15)$$

where $\varepsilon_c = \alpha_c \Delta T$ and $\varepsilon_s = \alpha_s \Delta T$ are the corresponding thermal strains, and α_c and α_s are arbitrarily assigned coating and membrane coefficients of thermal expansion (CTE). An increase in temperature ΔT provides via Eq. (15) corresponding increases in the intrinsic stresses. The relevant material and geometrical properties used in the model are shown in Table 1. (Note the negative CTE of the membrane, required to simulate a tensile intrinsic membrane stress.)

After specifying the membrane and coating stresses, the mirror was subjected to a 1-*g* gravity load (again, acting in the upward axial direction). This load produced a 7.86-mm displacement of the apex from its initial position. The resulting rms error was then calculated for the shape of the deformed mirror (Fig. 6), with the reference parabola defined as one passing through both the deformed apex position and outer boundary. Figure 6 shows that an rms error of ≈ 2.8 mm is caused by the 1-*g* loading and is invariant with the levels of intrinsic stress in the membrane and coating (chosen always to satisfy the 0-*g* ondesign coating prescription), indicating a lack of stress stiffening. Note that this is the rms error from a reference parabola passing through the deformed apex and outer boundary. The rms error for a reference parabola defined by the initial parabolic shape is roughly 2.5 times as large at 6.7 mm. Both of these numbers are important because the second quantifies the error from the original configuration and the former quantifies the residual error after the mirror deforms.

The described procedure was repeated for 1-, 5-, 10-, and 15-m-diam mirrors to investigate any size effects. First, it was found that, as for the 20-m mirror, the gravity sag rms errors are independent of the intrinsic stress values. Figure 7 shows the resulting rms errors referenced from the deformed configuration, as the mirror diameter is increased. A 9.3-μm rms error results for a 1-m-diam mirror. The rms error shown in Fig. 7 can be curve fit nearly perfectly to the mirror diameter by a parabola (with an r^2 value of 0.9997). The reason for an increased rms error for the larger mirror is an increase in the amount of material subjected to the gravitational body force, which also increases with the square of the mirror diameter.

Next, it was speculated that an increasing amount of intrinsic stress would allow greater communication of outer boundary manipulations to the rest of the mirror. Previous work has shown that boundary manipulations can be used to obtain a more parabolic shape.[21,22] Thus, boundary manipulations provide an additional degree of freedom to fine-tune the shape of the mirror. Better communication of outer boundary manipulations across the entire surface is also desirable. As was done earlier, the membrane shrinkage strain was allowed to vary from 0 to 1% in increments of 0.1%. The outer boundary of the 20-m mirror was then displaced

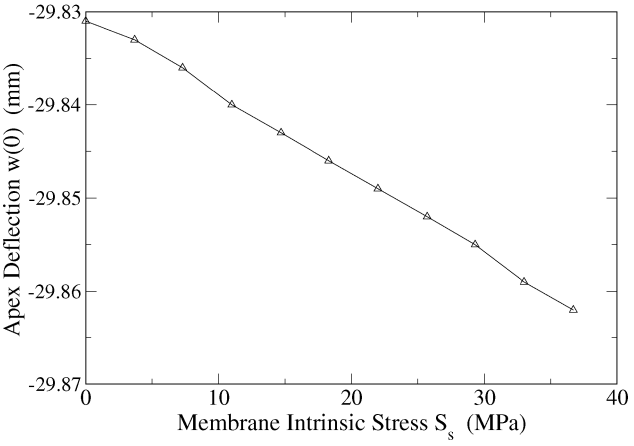

Fig. 8 Apex deflection of 20-m-diam, *f*/2 mirror, 0-*g* ondesign case subjected to a 0.02% outer boundary displacement.

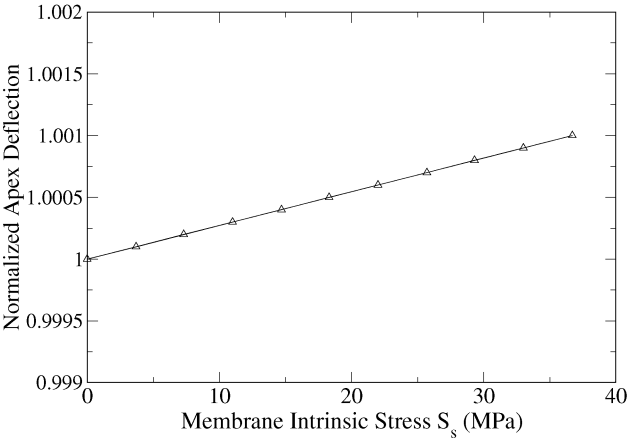

Fig. 9 Normalized apex deflection of a 20-m-diam, *f*/2 mirror, 0-*g* ondesign case subjected to a 0.02% outer boundary displacement.

radially by 0.002 m, and the resulting apex deflection was determined (Fig. 8). These data were normalized in Fig. 9 by dividing the apex deflection by the apex deflection obtained with no intrinsic stresses. Figures 8 and 9 show that there is a slight increase in the amount of radial boundary displacement information that is communicated through the mirror to the apex as a result of increasing intrinsic stresses. The largest amount of intrinsic stress imparted to the membrane and coating resulted in a 0.1% increase in the apex displacement.

Again, the issue of size effect was addressed by looking at the results for 1-, 5-, 10-, 15-, and 20-m-diam mirrors. Here, the boundary

displacement was kept to the same fixed percentage (0.02%) of the radius, for each diameter value. Figure 10 shows the resulting apex deflections with no intrinsic stress present. As is evident, a linear relation exists between the apex deflection and the mirror diameter, with 30 times the apex deflection for the 20-m mirror compared to the 1-m mirror.

Discussion

The results of the finite element analysis imply that a stress-stiffening effect is not present for an ondesign 0-g mirror when it is subjected to a 1-g gravity load, over the range of shrinkage stress examined. Only a slight effect is observed when the mirror is subjected to outer boundary displacements in a 0-g environment. After pondering a physical explanation for this behavior, it was determined that it was due to a lack of internal forces within the laminate mirror. Consider a planar membrane that is subjected to 1-g loading, again acting upward to be consistent with the curved mirror orientation. Under the action of gravity, the planar membrane attains some central sag. If this membrane is subjected to a radial boundary displacement, additional meridional forces are generated within the membrane, which act to reduce the amount of central sag. This is one feature that is desired with the applied stress coatings. To verify this to be the case, four initially planar models were investigated, which are described in Table 2. Note that the final diameter of each mirror is 20.01 m; hence, the 1-g gravititational load is applied in each case to a mirror of this diameter. It was expected that the first and second models would have the same apex displacements because the intrinsic stress in the second model was adjusted to be equivalent to the amount of stress induced by the radial boundary displacement of the first model. The third and fourth models were also expected to have the same apex displacements, due to the lack of internal forces in each case. The resulting apex displacements predicted by ABAQUS are shown in Table 2. We found that the apex displacements for cases 1 and 2 were slightly different, whereas those of cases 3 and 4 were, as expected, equal. It was determined that the slight difference in cases 1 and 2 was a result of the difference between true strain ε and engineering strain ε_0, where true strain is defined as $\varepsilon = \ell_n(1+\varepsilon_0)$. ABAQUS works with true strain, so that the radial displacement of 0.005 m used in case 1 (which induced an engineering strain $\varepsilon_0 = u(a)/a = 0.005/10 = 5\times10^{-4}$) corresponds to a true strain $\varepsilon = 4.99875\times10^{-4}$. When $\alpha\Delta T$ was set equal to the true strain value in case 2, we found the ABAQUS predictions for cases 1 and 2 to be the same. These results show that a stress-stiffening effect does not occur for a mirror satisfying the 0-g ondesign coating prescription, which we ascribe to the lack of net internal forces. When the intrinsic stresses produce a net internal force that mimics, for example, what occurs during radial boundary manipulation, then a stress-stiffening effect is observed as in case 2.

Table 2 Apex displacement $w(0)$, four initially planar cases

Case number	Case description	$w(0)$, m
1	20-m-diam, radial boundary displacement $u(a) = 0.005$ m, 1-g load	0.09718
2	20.01-m-diam, uniform shrinkage strain $\alpha\Delta T = -5\times10^{-4}$ m/m, 1-g load	0.09716
3	20.01-m-diam, 0-g ondesign coating stress, 1-g load	0.2067
4	20.01-m-diam, 1-g load only	0.2067

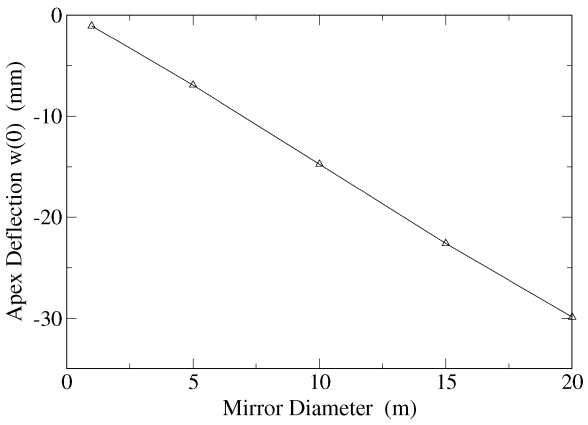

Fig. 10 Size effect for 0-g ondesign mirrors subjected to 0.0002a boundary displacement for diameters of $2a$ = 1, 5, 10, 15, and 20 m.

Another interesting point to consider is the amount of deformation occurring under a 1-g load for an initially curved vs an initially planar model. First, the case 4 data were reanalyzed for a 20-m (rather than 20.01-m) mirror for comparison with Fig. 6 data. An apex deflection of 206.6 mm was observed for this planar case, whereas an apex deflection of only 7.86 mm was observed for an initially parabolic mirror of the same diameter. This is roughly 26 times more deflection for the flat mirror, compared to its curved counterpart. Thus, although there is no stress stiffening (as confirmed by Fig. 6), it appears that there is a curvature-induced (geometric) stiffening as expected.

Conclusions

Expressions for the displacement fields of an initially curved shell laminate subject to intrinsic stresses were given. These equations yield results that are in excellent agreement with geometrically linear finite element results. A unique condition emerges when the coating stress and membrane stress satisfy a geometry-dependent relation. When this condition is satisfied, zero deformation results on removing the membrane from the mold that it was cast and coated on. The coating stresses in effect counteract the membrane shrinkage stresses. This provides what we have referred to as an ondesign coating prescription, given the thicknesses of each layer and the membrane shrinkage stress or strain. It applies to a 0-g environment, but alternative expressions were also given for a 1-g environment.

This 0-g ondesign coating prescription forces the stress resultants in the membrane and coating to equate to zero so that no displacements occur on removal from the mold. Thus, although there are nonzero intrinsic stresses in the coating and membrane, there is no net internal force within the laminate material. As a consequence of this lack of internal forces in the laminate, there is no stress-stiffening effect in the mirror when subjected to a 1-g load.

However, our theoretical results suggest that the coating stress can be adjusted to counteract additional forces. For example, under the 1-g loading condition, the mirror designed for 0-g will deflect under the gravitational body force. If the coating stress is then increased to a level defined by Eq. (14), the mirror will maintain the parabolic shape on removal from the mold. Thus, in this sense, stress stiffening has occurred.

Acknowledgments

We express our appreciation for the support provided by the Directed Energy Directorate of the U.S. Air Force Research Laboratory. We thank Daniel Segalman and Dean Mook, Program Managers in Structural Mechanics, Air Force Office of Scientific Research, for their support of this work.

References

[1]Freeland, R. F., "History of Relevant Inflatable High-Precision Space Structures Technology Developments," *Gossamer Spacecraft: Membrane and Inflatable Structures Technology for Space Applications*, edited by C. H. Jenkins, Vol. 191, Progress in Astronautics and Aeronautics, AIAA, Reston, VA, 2001, Chap. 2, pp. 35–47.

[2]Marker, D. K., Wilkes, J. M., Carreras, R. A., Rotgé, J. R., Jenkins, C. H., and Ash, J. T., "Fundamentals of Membrane Optics," *Gossamer Spacecraft: Membrane and Inflatable Structures Technology for Space Applications*, edited by C. H. Jenkins, Vol. 191, Progress in Astronautics and Aeronautics, AIAA, Reston, VA, 2001, Chap. 4, pp. 111–201.

[3]Gruneisen, M. T., Peters, K. W., and Wilkes, J. M., "Compensated Imaging by Real-Time Holography with Optically Addressed Spatial Light Modulators," *Proceedings of the SPIE: Liquid Crystals*, edited by I.-C. Khoo, Vol. 3143, Society of Photo-Optical Instrumentation Engineers, Bellingham, WA, 1997, pp. 171–181.

[4]Gruneisen, M. T., Martinez, T., and Lubin, D. L., "Dynamic Holography for High-Dynamic-Range Two-Dimensional Laser Wavefront Control," *Proceedings of the SPIE: High Resolution Wavefront Control: Methods Devices, and Applications III*, edited by J. D. Gonglewski, M. A. Vorontsov, and M. T. Gruneisen, Vol. 4493, Society of Photo-Optical Instrumentation Engineers, Bellingham, WA, 2002, pp. 224–238.

[5]Gruneisen, M. T., Dymale, R. C., Rotgé, J. R., and Lubin, D. L., "Near-Diffraction Limited Compensated Imaging and Laser Wavefront Control with Programmable Diffractive Optics," *Proceedings of the SPIE: High Resolution Wavefront Control: Methods Devices, and Applications IV*, edited by J. D. Gonglewski, M. A. Vorontsov, M. T. Gruneisen, S. R. Restaino, and R. K. Tyson, Vol. 4825, Society of Photo-Optical Instrumentation Engineers, Bellingham, WA, 2002, pp. 147–157.

[6]Carreras, R. A., Marker, D. K., Rotgé, J. R., Wilkes, J. M., and Duneman, D., "Deployable Near-Net-Shaped Membrane Optics," *Proceedings of the SPIE: High-Resolution Wavefront Control: Methods, Devices, and Applications*, edited by J. D. Gonglewski and M. A. Vorontsov, Vol. 3760, Society of Photo-Optical Instrumentation Engineers, Bellingham, WA, 1999, pp. 232–238.

[7]Stoney, G. G., "The Tension of Metallic Films Deposited by Electrolysis," *Proceedings of the Royal Society (London)*, Vol. A82, 1909, pp. 172–175.

[8]Brenner, A., and Senderoff, S., "Calculation of Stress in Electrodeposits from the Curvature of a Plated Strip," *Journal of Research of the National Bureau of Standards*, Vol. 42, Feb. 1949, pp. 105–123.

[9]Harper, B. D., and Wu, C.-P., "A Geometrically Nonlinear Model for Predicting the Intrinsic Film Stress by the Bending-Plate Method," *International Journal of Solids and Structures*, Vol. 26, No. 5/6, 1990, pp. 511–525.

[10]Hyer, M. W., "Calculation of the Room-Temperature Shape of Unsymmetric Laminates," *Journal of Composite Materials*, Vol. 15, July 1981, pp. 296–310.

[11]Masters, C. B., and Salamon, N. J., "Geometrically Nonlinear Stress-Deflection Relations for Thin Film/Substrate Systems with a Finite Element Comparison," *Journal of Applied Mechanics*, Vol. 61, Dec. 1994, pp. 872–878.

[12]Masters, C. B., Salamon, N. J., and Fahnline, D. E., "Deflection Shapes Due to Intrinsic Stress in Thin Films," *Materials Research Society Symposium Proceedings: Thin Films: Stresses and Mechanical Properties II*, Vol. 188, Materials Research Society, Pittsburgh, PA, 1990, pp. 21–27.

[13]Fahnline, D. E., "Effect of Initial Substrate Curvature on Nonlinear Bending Measurements of Thin-Film Stress," *Materials Research Society Symposium Proceedings: Thin Films: Stresses and Mechanical Properties III*, Vol. 239, Materials Research Society, Pittsburgh, PA, 1992, pp. 251–256.

[14]Chung, H., Lee, C., and Han, H., "Moisture-Induced Stress Relaxation of Polyimide Thin Films," *Polymer*, Vol. 42, No. 1, 2001, pp. 319–328.

[15]Lee, S. H., and Bae, Y. C., "Thermal Stress Analysis for Polyimide Thin Film: The Effect of Solvent Evaporation," *Macromolecular Theory and Simulations*, Vol. 9, No. 5, 2000, pp. 281–286.

[16]Pecht, M., Wu, X., Paik, K. W., and Bhandarkar, S. N., "To Cut or Not to Cut: A Thermomechanical Stress Analysis of Polyimide Thin-Film on Ceramic Structures," *IEEE Transactions on Components, Packaging, and Manufacturing Technology–Part B*, Vol. 18, No. 1, 1995, pp. 150–153.

[17]Wilkes, J. M., "Mechanics of a Near Net-Shape Stress-Coated Membrane. Volume I: Theory Development Using the Method of Asymptotic Expansions," U.S. Air Force Research Lab., Technical Rept. AFRL-DE-TR-2002-1063, Vol. 1, Kirtland AFB, NM, Dec. 2002.

[18]Wittrick, W. H., "Stability of a Bimetallic Disk: Part I," *Quarterly Journal of Mechanics and Applied Mathematics*, Vol. 6, 1953, pp. 15–26.

[19]Wilkes, J. M., "Mechanics of a Near Net-Shape Stress-Coated Membrane. Volume II: Boundary Value Problems and Solutions," U.S. Air Force Research Lab., Technical Rept. AFRL-DE-TR-2002-1063, Vol. 2, Kirtland AFB, NM, June 2003.

[20]Reicher, D. W., and McCormack, S. A., "Production of Thin Film Coatings with Predetermined Stress Levels," *Proceedings of the SPIE: Imaging Technology and Telescopes*, edited by J. W. Bilbro, J. B. Breckinridge, R. A. Carreras, S. R. Czyzak, and M. J. Eckart, Vol. 4091, Society of Photo-Optical Instrumentation Engineers, Bellingham, WA, 2000, pp. 104–111.

[21]Jenkins, C. H., and Marker, D. K., "Surface Precision of Inflatable Membrane Reflectors," *Journal of Solar Energy Engineering*, Vol. 120, No. 4, 1998, pp. 298–305.

[22]Ash, J. T., Jenkins, C. H., and Marker, D. K., "Deployment of a Membrane Mirror with an Axial Plunger," AIAA Paper 2000-1812, April 2000.

M. S. Lake
Associate Editor